

No part of this digital document may be reproduced, stored in a retrieval system or transmitted commercially in any form or by any means. The publisher has taken reasonable care in the preparation of this digital document, but makes no expressed or implied warranty of any kind and assumes no responsibility for any errors or omissions. No liability is assumed for incidental or consequential damages in connection with or arising out of information contained herein. This digital document is sold with the clear understanding that the publisher is not engaged in rendering legal, medical or any other professional services.

Chapter 12

HIGH LOAD POLYPROPYLENE COMPOSITES

*L. Fambri^{*1}, D. Lorenzi¹, E. Masarati² and E. Costantini²*

¹Department of Industrial Engineering, University of Trento,
via Mesiano, Trento, Italy

²Basell Poliolefine Italia srl a company of Lyondellbasell,
“G. Natta” R&D, P.le L. Donegani, Ferrara, Italy

ABSTRACT

Polypropylene composites with high content of inorganic filler or short glass fiber could be produced after compounding in a single screw Buss technology or in a twin-screw extruder. Specific formulations were properly prepared to guarantee an adequate processability for injection molding or extrusion. Polypropylene matrix was a proper combination of low and high melt flow grades in the range of about 3-12 g/10min and 500-2300 g/10min respectively. High content polypropylene composite containing up to 60% by wt. of talc, 80% of calcium carbonate or 65% of short glass were produced using a relatively low viscosity matrix.

Good flow-ability and processability for all compositions were evidenced. ISO specimens and large plates obtained after injection molding evidenced the increase of stiffness, strength, toughness at low temperature, and reduction of shrinkage. Deep investigation was conducted on glass fiber composites at 40-50-60%. (DSC, TGA, SEM, DMA, fiber distribution, flammability evaluation, and comparison). Results have been discussed and correlated with the compositions.

INTRODUCTION

Reinforced polypropylene (PP) materials represent one of the high volume production compounds for a large variety of applications where improvement of stiffness, strength and increase of heat deflection temperature are required. Moreover, the significant decrease of the relative price becomes a strategic factor. Three fillers are the most considered due to

* E-mail address: Luca.Fambri@ing.unitn.it

favorable combination of properties, processing [1] and costs: talc, calcium carbonate, and glass fiber.

However, some limitations must be considered, especially in polypropylene composite with a high percentage of filler, due to the reduction of other properties such as the impact strength, deformation at break, and critical problems in processing conditions like injection molding. Hence, because of the increase in melt viscosity for general applications, typical percentages reach about 20-40% by wt. for particulate filler and about 30% by wt. of glass fiber [2-4].

Concerning production and applications, the market of glass fiber polypropylene composites represents a significant and technical sector with respect to polypropylene resins. According to recent data, in 2010 the European polypropylene resins sales reached 9.9Mtons, as result of 7.5 Mtons in Western Europe and 2.4 Mtons in Central/Eastern Europe [5]. And concerning glass fiber reinforced polypropylene, European sales in 2009 required 160 ktons as reported in Table 1 and are expected to largely increase in the coming years. The main application sector is automotive, followed by electrical and electronics, furniture and other segments (Non automotive).

It is interesting to underline that the production of polypropylene composite granule is distinguished in short glass fiber up to about 2-4 mm (SGF) and long glass fibers up to 8-15 mm (LGF), with 2009 consumptions in the proportions of about 67% and 33%, respectively.

Literature reveals papers and publications of researchers dealing with the properties of short glass fibers polypropylene composite [6-20] in dependence on the characteristics of the matrix, the type and content of fibers, their average length and distribution, the presence of any adhesion promoter, the processing conditions, and the final shape of the required/desired item.

Table 1. Glass reinforced PP compound consumption in Europe by ktons [5]

Application sector	Year	2006	2009	2014
Automotive		110	100	160
Non Automotive		80	60	75
	Total	190	160	235

On the other hand, recent developments suggested the use of long glass fiber in reinforced polypropylene to improve mechanical properties, such as impact resistance and creep behavior [21-28]. It should be taken into account that several factors affect the final properties, as result of a combined effect of the composition and processing conditions (injection molding and mold design).

Moreover, attention is specifically dedicated to the fiber orientation in dependence on the processing conditions in extrusion and injection, and its direct effects on the composite properties [29-50]. In all cases, a critical problem, especially for long glass fibers, is the severe fiber breakage occurring in injection molding, determining processed composites with shorter fiber length distribution [51-56].

Following these general considerations, the study of preparation, processing, and the characterization of high load polypropylene composites will be described/treated in this chapter with particular relevance on the short glass fibers polypropylene composites up to 40-60% by wt. It should be underlined for this purpose that a specific selection of polypropylene

matrix was necessary to overcome the effects of high viscosity after filler addition in compounding and specimens processing.

MATERIALS AND SAMPLE PREPARATION

Isotactic polypropylene (iPP) is a product of LyondellBasell. Four polymers with different melt flow rate (MFR) at high and low grade were selected and coded, as in the following. PP2300 is a homopolymer with a MFR of 2300 g/10 min; PP550 is a homopolymer with a MFR of 550 g/10 min; PP12 is a homopolymer with a MFR of 12 g/10 min; PP3 is a random copolymer with a MFR of 3 g/10 min and containing 1.6 % of ethylene.

Polybond 3200, a polypropylene homopolymer, grafted with about 1% of maleic anhydride (PP-g-MA) and MFR 115 g/10 min, and commercialized by Chemtura, was used as coupling agent (CA) in glass fiber composites with a GF/CA ratio of 20, in line with what also described elsewhere [57-58].

Two type of talc at medium and fine size particles fillers were: Luzenac HAR T84 from Imerys-France (T1), a High Aspect Ratio Talc with aspect ratio of about 10-20 vs. 3-5 of a standard talc and HM05 from IMI Fabi SpA-Italy (T2) with more than 95% of particles lower than 5 μm .

Calcium carbonate (CC) Omyacarb 2T-UM was supplied by Omya SpA-Italy (more than 32% have particles lower than 2 μm , and more than 99% lower than 45 μm).

Short glass fiber (SGF) with density 2.65 g/cm³, diameter of 13 μm and average length of 3 mm was selected (Fibre Glass ECS O3T 480, from NEG-Japan).

Composites with particulate fillers (Table 2) were prepared using a single screw extruder, Buss kneader technology model MDK70 (oscillating screw shaft), with screw diam. 70 mm and L/D = 17. Inorganic fillers were fed into the melt polypropylene through second vertical feeding ports. Running conditions were screw speed = 270 rpm, capacity = 50-60 kg/h and barrel temperature = 200-230 °C.

Table 2. Composition of particulate polypropylene composites

Matrix and Filler (%)	T40	T50	T60	CC80
PP 2300 Homopolymer	-	25	27	13
PP 12 Homopolymer	40	-	13	-
PP 3 Random Copolymer	-	25	-	7
PP 550 Homopolymer	20	-	-	-
Talc (T1)	-	50	60	-
Talc (T2)	40	-	-	-
Calcium Carbonate (CC)	-	-	-	80

Glass fiber composites (Table 3) were prepared using a twin screw extruder model Werner and Pfeiderer ZSK40SC with a screw diam. 40 mm and L/D = 43 provided with gravimetric feeders; polypropylene and a coupling agent were fed into the first barrel, and the short glass fiber was fed into the fifth barrel via forced side feeding. Running conditions were screw speed = 200 rpm, capacity = 50-60 kg/h and barrel temperature = 200-220 °C.

Table 3. Composition of fibrous polypropylene composites

Matrix and Filler (%)	GF40	GF45	GF50	GF55	GF60	GF65
PP 2300 Homopolymer	-	17.6	23.75	14.1	18.5	15.85
PP 12 Homopolymer	58	17.6	-	14.1	-	-
PP 3 Random Copolymer	-	17.6	23.75	14.1	18.5	15.85
Polybond 3200	2	2.2	2.5	2.7	3	3.3
Glass Fiber (GF)	40	45	50	55	60	65

For determination of materials properties, T-bar specimens ISO 527-1 type 1A (length: 170 mm; thickness: 4.0 mm; gauge length: 80 mm; gauge width: 10 mm) were prepared by injection molding following ISO 1873-2 (2007) by using a Negri-Bossi injection molding machine (melt temperature: 230-270°C; injection pressure: 30-60 MPa; mold temperature: 50°C).

Selected composites were also injection molded to produce large plates (length: 250 mm; width: 150 mm; thickness: 3.2 mm) in a specific mold provided by a film gate 1.5 mm thick and 150 mm wide.

CHARACTERIZATION METHODS

Density was measured according to ISO 1183-2:2004 (Part 2: Density gradient column method).

Melt flow rate (MFR) was performed on the produced composites by using the instrument Melt Flow Index LMI 4000 (Dynisco) according to ISO 1133:2005 with a load of 2.16 kg at 230°C.

Spiral flow test were performed using an injection molding machine by Sandretto Model 190 with a clamping force of 1900 kN. Melt temperature of 230°C, injection pressure between 2 and 10 MPa, a single cavity endless spiral flow mold with 2.5 mm depth, and mold temperature of 40°C were selected as experimental conditions.

Heat deflection temperature (HDT) and Vicat softening temperature (VST) were determined by using a HDT-Vicat apparatus model MP3 (product of ATS-FAAR, Italy). HDT test was performed on T-bar specimens at 1.8 MPa following ISO 75A. VST was measured according to ASTM D1525-00 with a load of 10 N and a heating rate of 120°C/h. The dimensions of test specimens prepared from the plates were 12 mm x 12.8 mm x 3.2 mm.

Mechanical properties were determined at room temperature (23°C) by using a dynamometer Instron mod.4502 in bending and tensile mode at 50 mm/min, according to ISO178 and ISO527, respectively. Tensile modulus (secant) was determined with gauge length of 1 mm/min and span of 50 mm.

Charpy tests were performed on unnotched and notched (Notch A) rectangular specimens 80x10x4 mm from T-bars following ISO 179 (type 1; edgewise).

Thermal degradation and composition of pure and GF reinforced polypropylene were studied in thermogravimetric analysis (TGA) using thermobalance Mettler TG 50 at a heating rate of 10°C/min in air flow of 100 ml/min in the range 50-700°C.

Differential scanning calorimetry (DSC) analysis was performed using a Mettler DSC30 calorimeter by using a cycle of heating-cooling-heating in the range 0-230°C at $\pm 10^\circ\text{C}/\text{min}$ flushing nitrogen at 100 ml/min. Melting temperature and crystallization temperature were reported. The crystallinity content was evaluated from the melting peak and referred to the value of 209 J/g for 100% crystalline polypropylene reported in literature [59].

Scanning electron microscopy (SEM) pictures were obtained by using a Philips® XL30 Environmental Scanning Electron Microscope at an acceleration voltage between 15 and 30 kV. Samples were fractured in liquid nitrogen and then fracture surface was metalized.

Measurements were performed using a Dynamic mechanical thermal analysis DMTA Mk II (Polymer Laboratories Ltd, Loughborough, UK). The storage E' and loss E'' moduli were measured in the single cantilever bending mode at frequency 1 Hz in the range -50 to 150°C (test pieces 19 mm x 5 mm x 3.2 mm were cut of the large plates; heating rate $3^\circ\text{C}/\text{min}$; dynamic displacement 0.064 mm). The glass transition temperature of the PP component was identified with the position of the maximum respective loss modulus peak on temperature scale. Effect of orientation was evaluated after tensile DMTA performed on rectangular specimens (19 mm x 2 mm x 3.2 mm) longitudinally and transversally cut of the large plate (static stress of 1 MPa). Longitudinal and transversal deformation (D) were calculated as $D = 100 \times \Delta L/L_0$, in dependence on the initial specimen length L_0 and the length variation ΔL . The coefficient of (linear) thermal expansion $\text{CTE} = (\Delta L/L_0)/\Delta T$ was calculated for three temperature intervals ΔT , by using the initial specimen length L_0 and the length variation ΔL over the selected interval ΔT .

RESULTS AND DISCUSSION

Preliminary analysis of compounded composites evidenced a suitable flowability for injection molding. Melt flow rate, as reported in Table 4 and 5, was found in the range between 1-82 g/10 min for particulate composites and 3-7 g/10 min for fibrous composites in dependence on the matrix and the filler content.

The density of composite increased linearly with the percentage of filler, reaching 1.51 g/cm^3 for 60% of talc, 1.82 g/cm^3 for 80% of calcium carbonate, and 1.56 g/cm^3 for 65% of SGF.

See Tables 2 and 3 for the composition, and Tables 4 and 5 for the properties of particulate and fibrous composites, respectively.

Table 4. Properties of particulate polypropylene composites

Properties	T40	T50	T60	CC80
Density (g/cm^3)	1.244	1.360	1.514	1.820
Melt Flow Rate (g/10min)	22.8	8.6	1.8	82
Tensile modulus (GPa)	5.17	7.50	9.60	6.65
Tensile strength (MPa)	37	39	31	20
Deformation at break (%)	2.2	1.5	1.3	1.0
Charpy unnotched (kJ/m^2)	13	10	3.4	3.4

Table 5. Properties of fibrous polypropylene composites

Properties	GF40	GF45	GF50	GF55	GF60	GF65
Density (kg/dm ³)	1.216	1.275	1.320	1.404	1.475	1.557
MFR (dg/min)	3.0	5.3	6.8	4.7	6.8	3.8
Tensile Modulus (GPa)	8.90	10.04	12.20	12.96	14.75	16.06
Strength at Break (MPa)	116	121	131	126	130	121
Elongation at Break (%)	2.4	2.5	2.4	1.7	2.2	1.6
Charpy unnotched (kJ/m ²)	59.5	61.2	63.4	49.4	44	40
Charpy unnot.-30°C (kJ/m ²)	63	67.5	67.6	57	57	41
HDT @1.8MPa (°C)	151	150	148	149	148	150

Glass fiber polypropylene composite revealed higher mechanical properties with respect to the correspondent filled with talc and calcium carbonate as shown in Table 5.

Moreover spiral flow test was performed on selected PP composites and evidenced a good processability for T40, and GF40 GF50, as depicted in Figure 1.

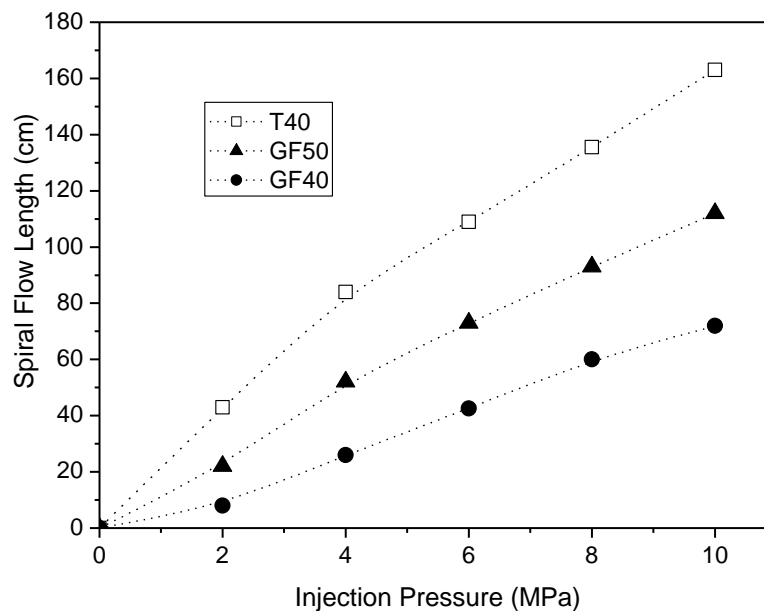


Figure 1. Effect of injection pressure at 230°C on spiral flow length of PP composite containing talc at 40% by wt. (□); short glass fiber at 50% (▲) and 40% by wt. (●).

It is well evident the effect of polypropylene matrix and the correspondent MFR.

As expected, higher values of flexural modulus and Notched Charpy test at 23°C were evidenced for short glass fiber composites with respect to particulate composites, as shown in Figure 2 and 3.

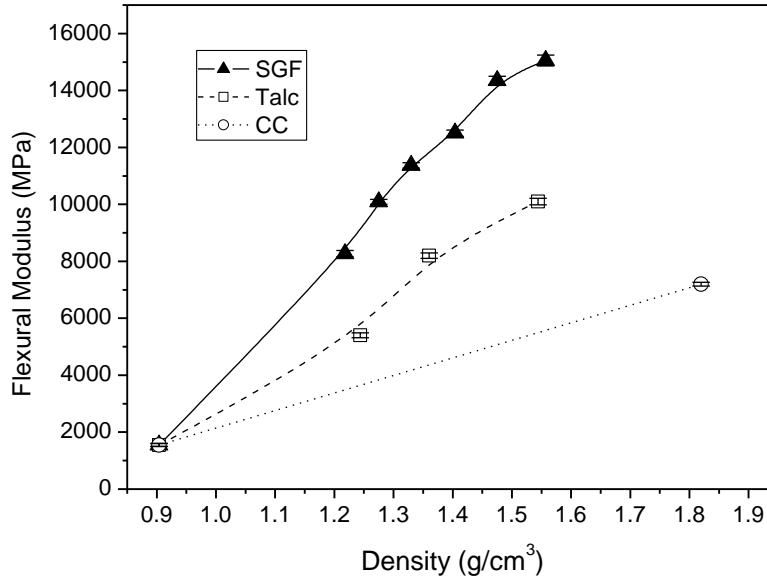


Figure 2. Effects of various filler content and density of PP composite on flexural modulus. Short glass fiber 40-65% by wt. (▲); talc 40-60% by wt. (□); calcium carbonate 80% by wt. (○).

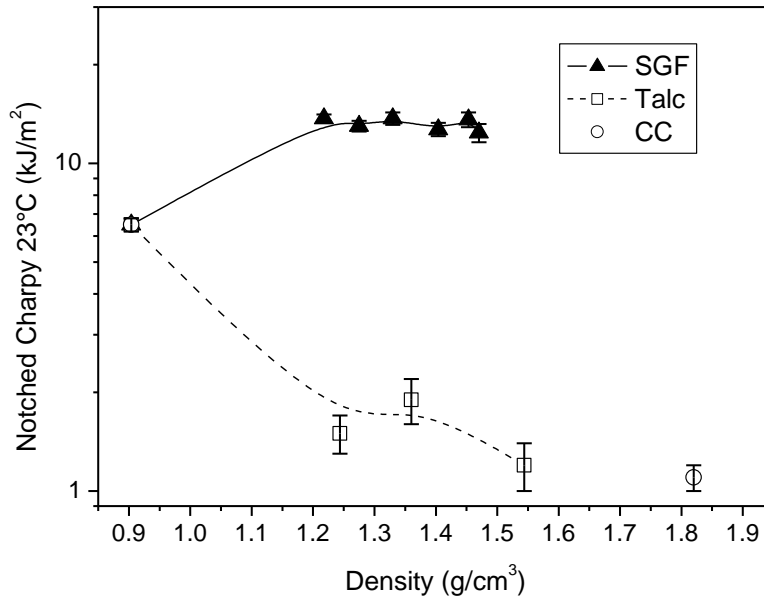


Figure 3. Effects of various filler content and density of PP composite on notched Charpy. Short glass fiber 40-65% by wt. (▲); talc 40-60% by wt. (□); calcium carbonate 80% by wt. (○).

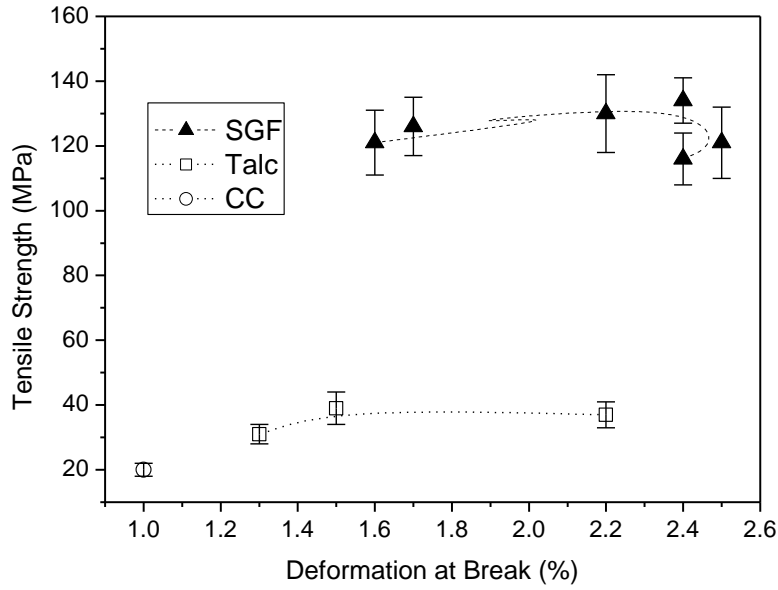


Figure 4. Effects of various filler content on tensile strength and deformation at break of PP composite. Short glass fiber 40-65% by wt. (▲); talc 40-60% by wt. (□); calcium carbonate 80% by wt. (○).

To better understand elastic properties, the tensile modulus (E_C) was evaluated using the traditional model for random oriented short fiber composites [60-61] according to equation I:

$$E_C = \frac{3}{8} E_L + \frac{5}{8} E_T \quad (\text{I})$$

where E_L and E_T are elastic moduli of the composite with longitudinal and transversal aligned fibers, respectively. These moduli can be calculated following the semi-empiric model Halpin-Tsai with the equations II-IV:

$$E_L = \frac{1 + 2(l/d)(\eta_L \phi)}{1 - \eta_L \phi} E_M \quad (\text{II})$$

$$E_T = \frac{1 + 2\eta_T \phi}{1 - \eta_T \phi} E_M \quad (\text{III})$$

and

$$\eta_L = \frac{(E_F / E_M) - 1}{(E_F / E_M) + 2(l/d)} \quad (\text{IVa})$$

$$\eta_T = \frac{(E_F / E_M) - 1}{(E_F / E_M) + 2} \quad (\text{IVb})$$

where l/d is the aspect ratio of the fibers, Φ is the volume fraction of the fibers, and E_F and E_M are the fiber and matrix moduli (70 GPa and 1.68 GPa, respectively).

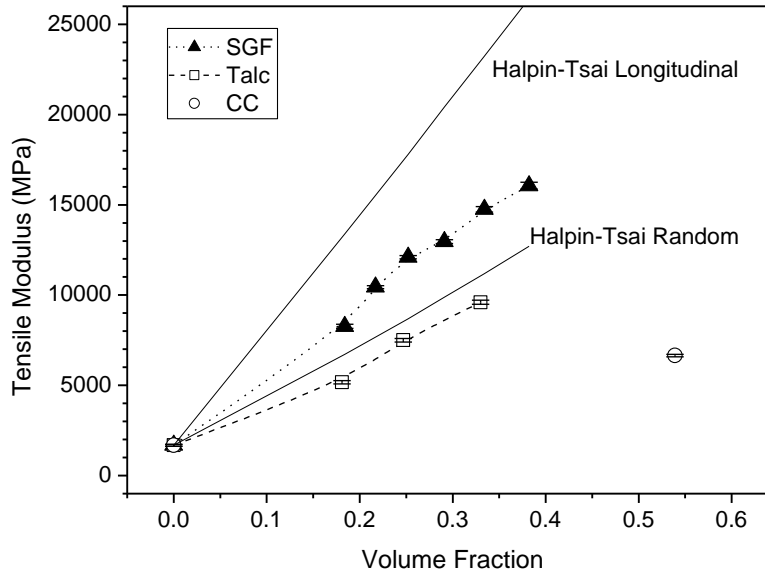


Figure 5. Tensile modulus of PP composites containing short glass fiber 40-65% by wt. (\blacktriangle); talc 40-60% by wt. (\square); calcium carbonate 80% by wt. (\circ), as function of volume fraction. Continuous lines represent the prediction according to Halpin-Tsai model for longitudinal and random oriented fiber composites.

Note that the Charpy test on notched specimens revealed at room temperature an almost constant energy to break of about 12-14 kJ/m² for all glass fiber polypropylene composites. On the other hand, at -30°C the energy to break is much higher and is directly proportional to the percentage of fiber content up to 65% by wt. (Figure 6).

Due to the higher properties, PP composites based on 40, 50 and 60% by wt. of short glass fiber were more deeply characterized. To avoid asymmetrical flow in injection molding, as shown by Karian and Stoops [38] in the case of single gate mold, the large rectangular plates were produced filling the mold cavity through a film gate 1.5 mm thick and 150 mm wide. These plates were used for TGA, DSC, DMTA analysis, and some tests to compare the material flammability.

DSC analysis evidenced in Figure 7 similar behavior of PP matrix and GF50 and GF60, for both crystallinities (44-45%), melting temperature (157-158°C) and crystallization temperature (112-115°C). Higher values were found for GF40, in dependence on the polypropylene composition.

TGA analysis confirmed the nominal composition, as shown in Figure 8, revealing a residual mass of about 37, 49 and 58% of glass fibers respectively. Two tests after longitudinal and transversal break were reported for each composition.

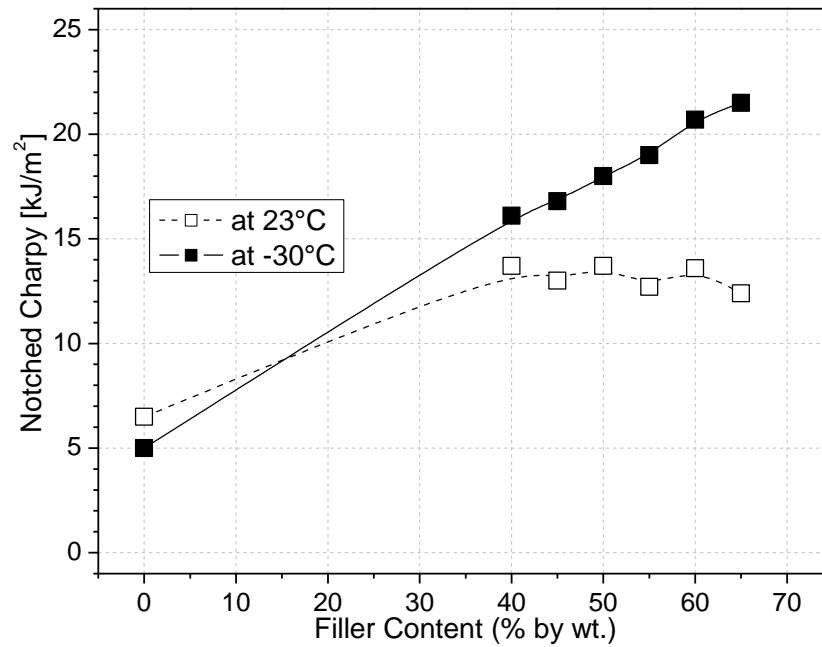


Figure 6. Notched Charpy test of SGF-PP composites at 23°C and -30°C.

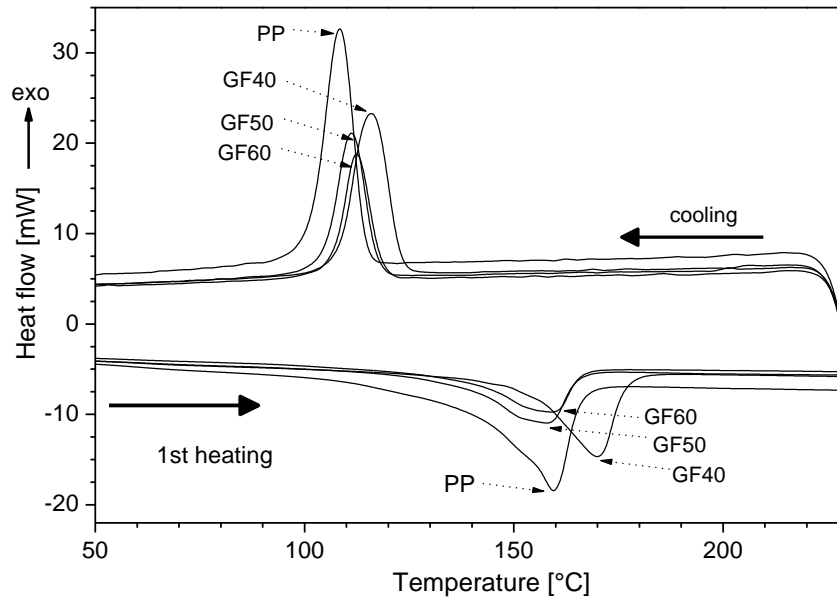


Figure 7. DSC thermograms of SGF-PP composites.

Table 6 reports some results of mechanical characterization at high temperature (flexural test at 80°C, creep experiments at 105°C), shrinkage evaluation according to standard or internal procedures, and thermal data.

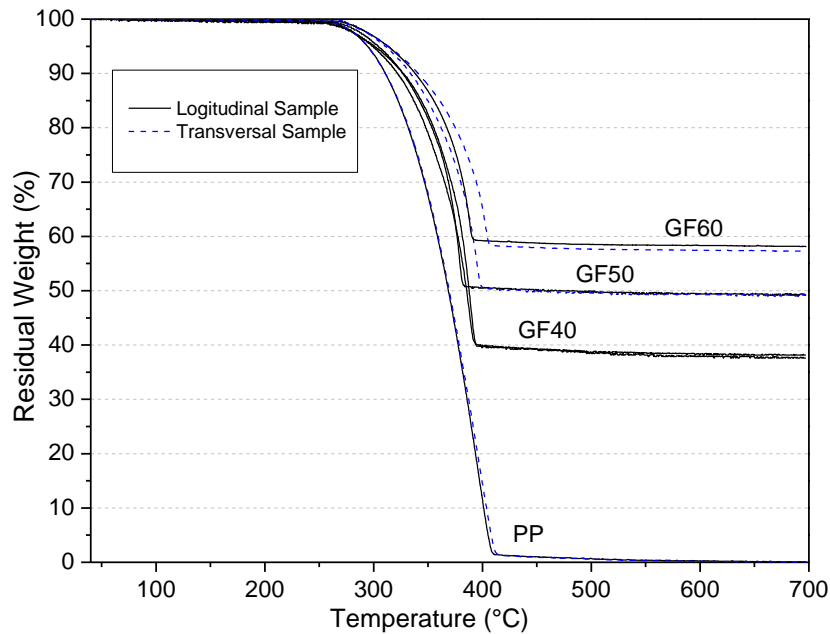


Figure 8. TGA thermograms of SGF-PP composites in air flow.

Table 6. Selected properties of SGF polypropylene composites

Properties	Method	GF40	GF50	GF60
Flexural Modulus @80°C (GPa)	ISO 178	5.05	7.20	8.80
Flexural Strength @80°C (MPa)	ISO 178	76	95	98.5
VST (°C)	ASTM D1525	158	146	152
Longitudinal Shrinkage (%)	Internal	0.21	0.09	-
Transversal Shrinkage (%)	Internal	0.87	0.55	-
Tensile Creep 105°C, 17MPa Time to Fracture (h)	ISO 899	41.5	58.5	-
Elongation to Fracture (%)	ISO 899	2.13	1.45	-
Polypropylene crystallinity (%)	DSC	48	44	45
Melting Temperature 1 scan (°C)	DSC	168	157	158
Crystallization Temperature (°C)	DSC	119	114	115
Melting Temperature 2 scan (°C)	DSC	166	154	155
Glass fiber content (%)	TGA	37	49	58
CLTE @ -40/-20°C ($10^{-6}/^{\circ}\text{C}$)	DMTA	9-24	13-25	13-18
CLTE @ 5/35°C ($10^{-6}/^{\circ}\text{C}$)	DMTA	15-52	34-54	16-33
CLTE @ 60/90°C ($10^{-6}/^{\circ}\text{C}$)	DMTA	11-61	46-84	20-69
Glass transition temperature (°C)	DMTA	7-8	5-6	7-8

Fiber Length Analysis and Distribution

About 30 mg of each GF/PP composition were thermally degraded in TGA crucible after heating in air flow up to 700°C. The residue was collected and undergone to optical image analysis. The fiber length measurements were made with the help of polarized light microscopy (Leitz Ortholux II POL-BK) and computer aided image analysis (ImageJ), as shown in Figure 9. The fiber length distribution (FLD) was determined by the average fiber length, which calculated from a minimum of 500 length measurements on fibers recovered from the incineration (Figure 10). As expected the curve distribution evidenced a much higher length reduction for the 50-60% GF PP composite with respect to the 40% GF content. Values of D50 and D90 were found in accordance to literature [56].

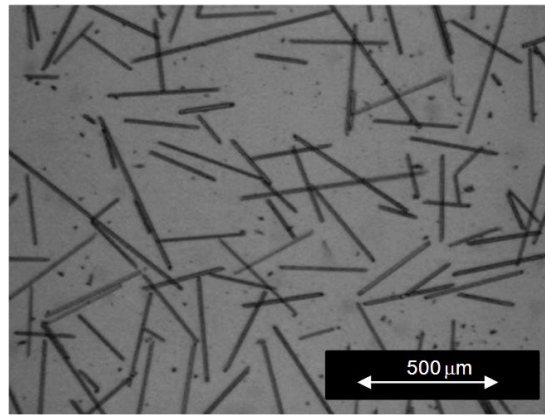


Figure 9. Fiber length analysis (Optical microscope).

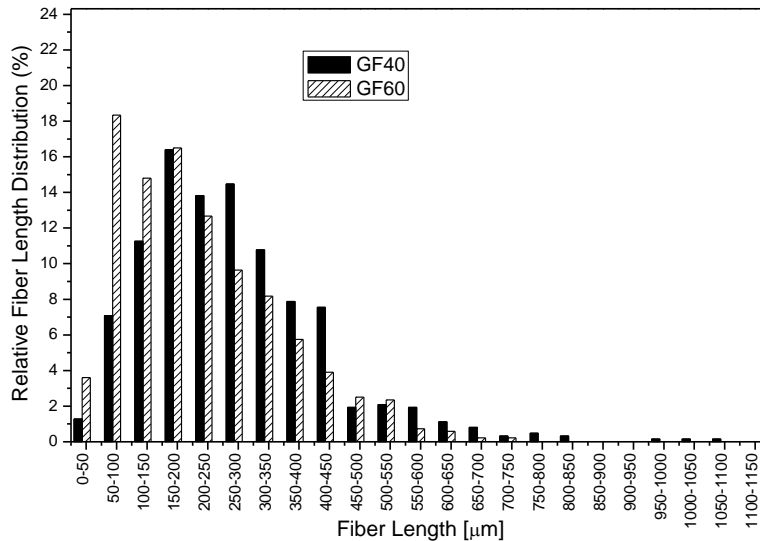


Figure 10a. Relative fiber length distribution in SGF PP composites.

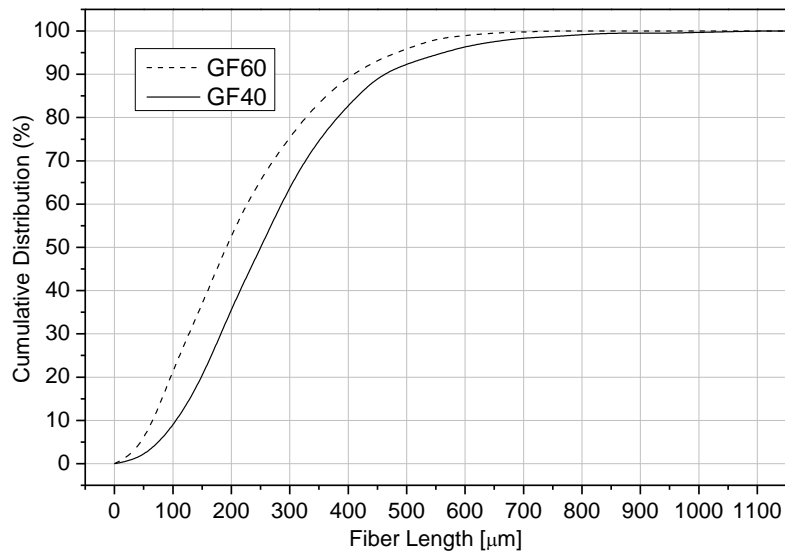


Figure 10b. Cumulative fiber length distribution in SGF PP composites.

Vicat softening temperature (50 N, 2°C/min) was increased from $106 \pm 5^\circ\text{C}$ of the i-PP matrix to $146 \pm 4^\circ\text{C}$ and $152 \pm 3^\circ\text{C}$ of iPP composites, at 50 and 60% SGF respectively, whereas higher VST $158 \pm 2^\circ\text{C}$ was found for 40%, directly dependent on matrix composition, as shown in Figure 11.

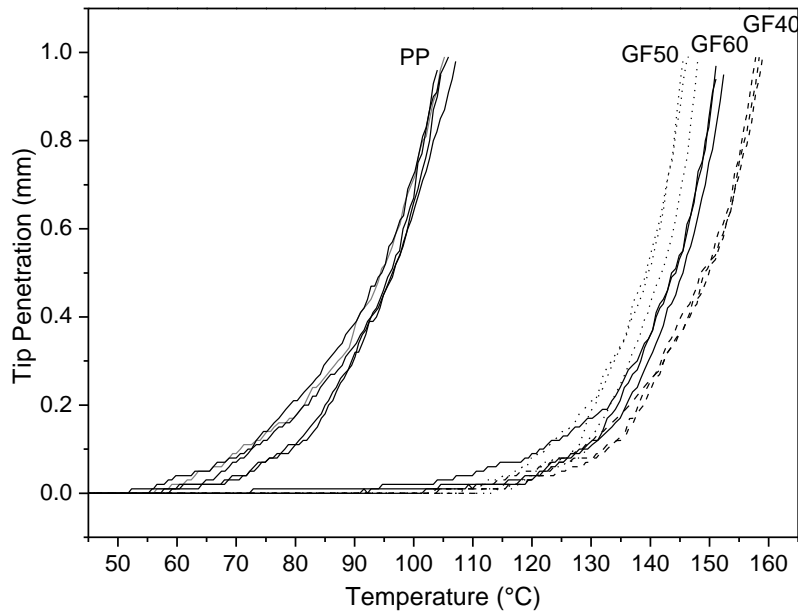


Figure 11. Vicat Test on PP and SGF-PP samples.

Higher stiffness and strength, and reduced shrinkage with better creep resistance were found as the most interesting improvements of the high-content SGF-iPP composites. On the

other hand, deformation at break, HDT and Charpy tests remained almost unchanged versus 40 % GF PP. For example, flexural modulus increased from about 9 GPa up to 12 and 14 GPa, for i-PP composites containing 40, 50 and 60% by wt of SGF respectively.

Bending DMTA analysis showed significant differences in storage modulus (Figure 12), depending on both SGF content and injection molding direction. Loss modulus data (Figure 13) reported a glass transition peak at about 5°C independently with a shoulder peak at around 60°C.

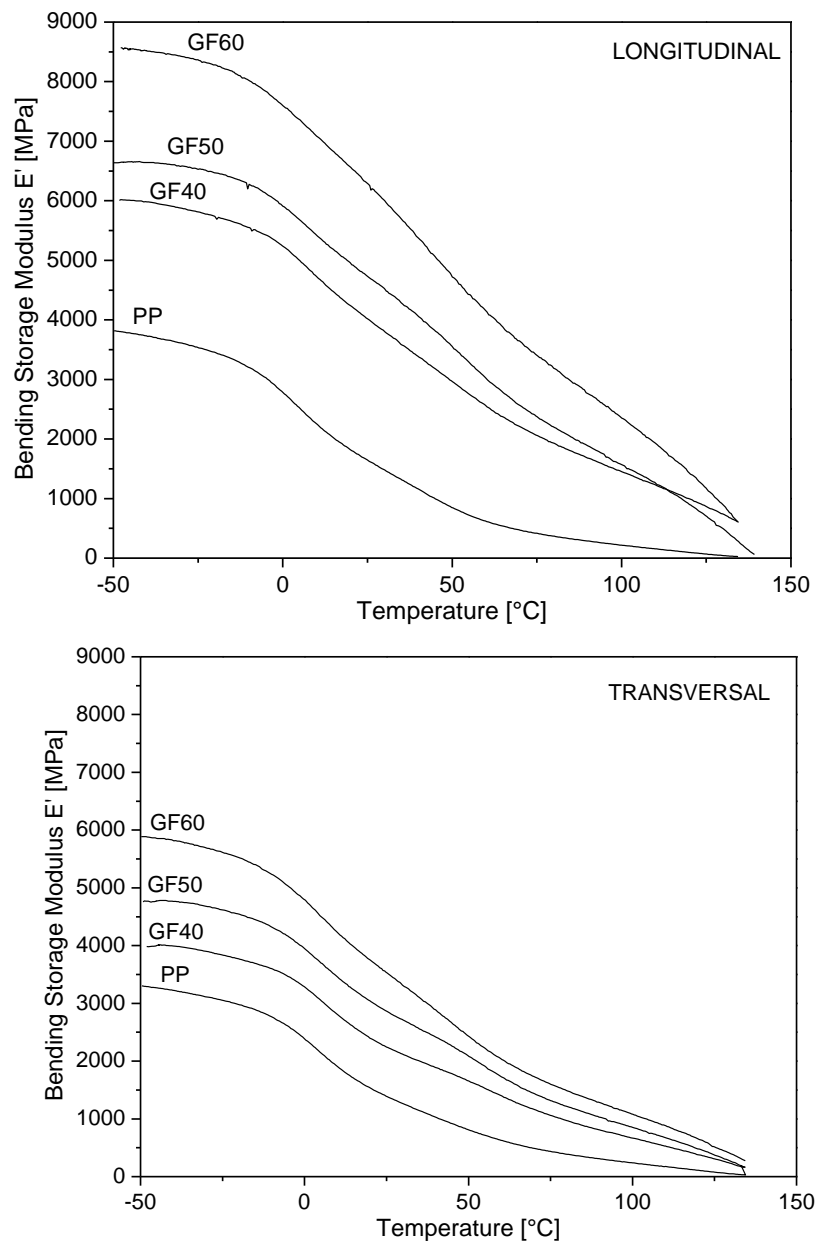


Figure 12. Bending storage modulus of PP composites as function of composition and longitudinal/transversal direction.

Specific analysis of the anisotropic properties of injection molded plates was obtained by comparing characterization of specimens machined in longitudinal and transversal directions, evidencing higher storage and loss modulus and lower tensile thermal deformation (Figure 14).

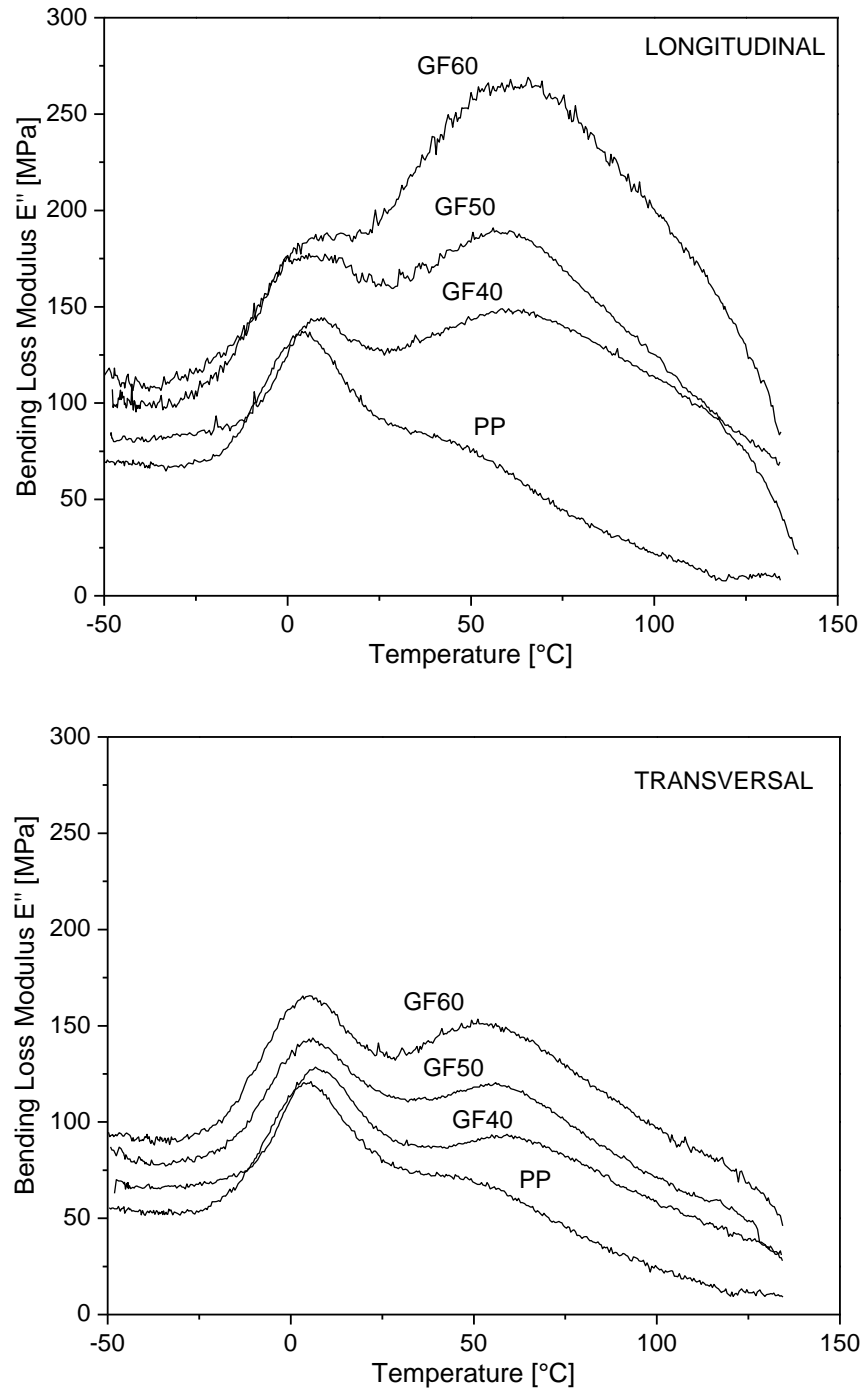


Figure 13. Bending loss modulus of PP composites as function of composition and longitudinal/transversal direction.

The anisotropy factor evaluated as the ratio between longitudinal storage modulus and transversal storage modulus is reported in Figure 15 as function of temperature.

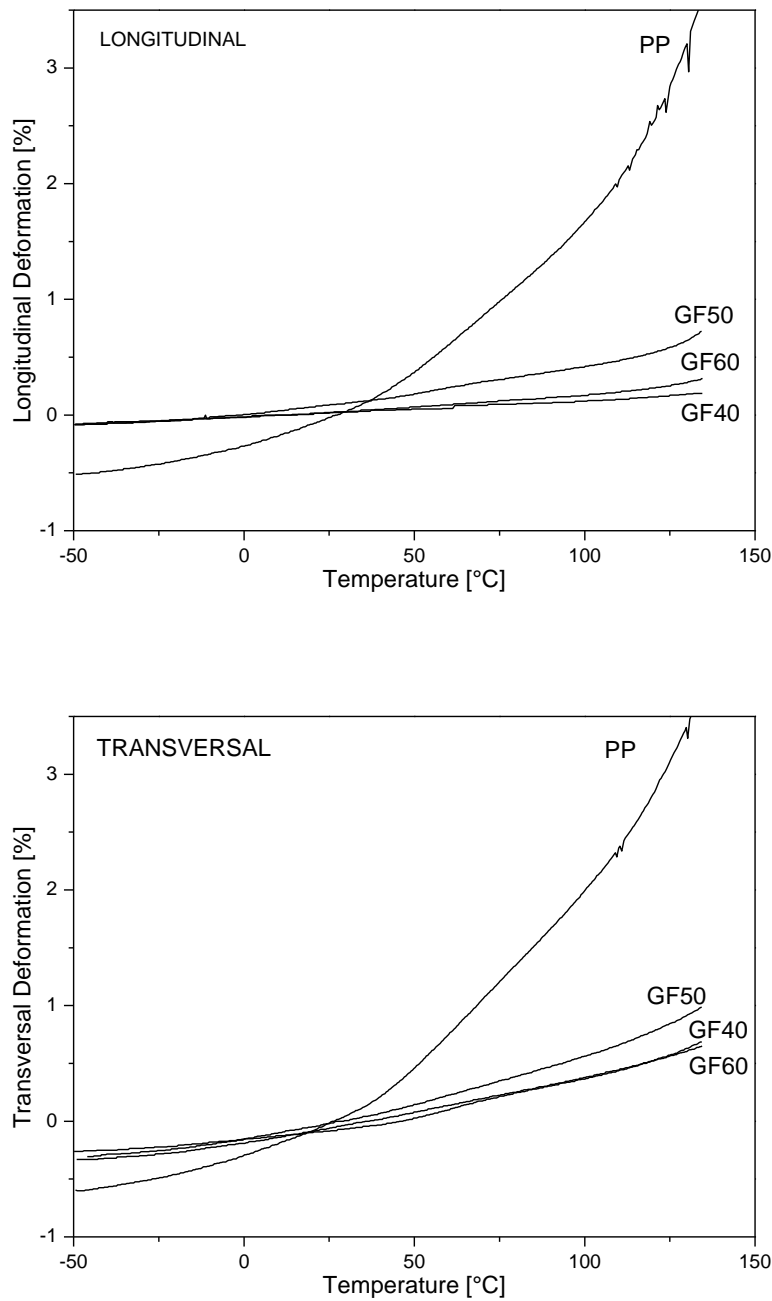


Figure 14. Thermal deformation during tensile DMTA test in longitudinal/transversal direction.

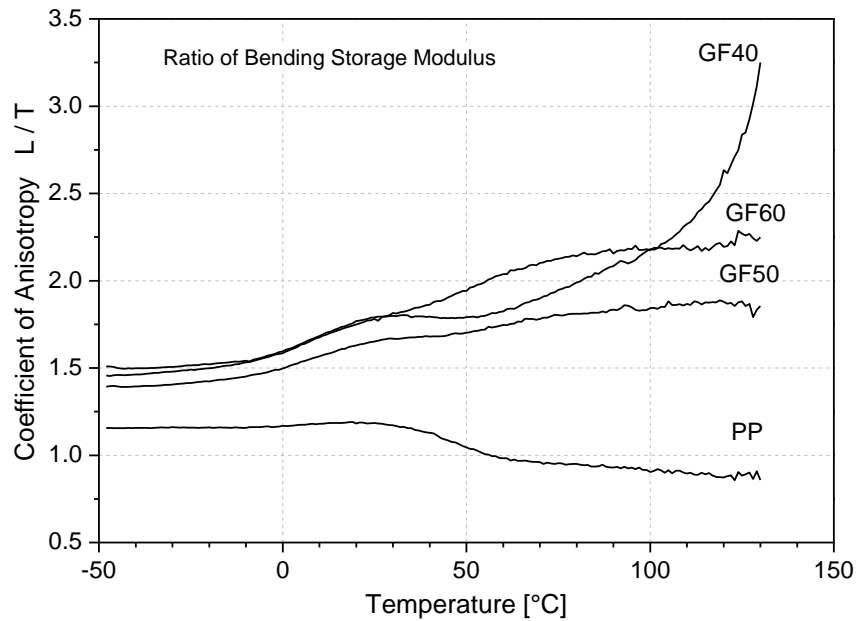


Figure 15. Anisotropy factor ($E'_{\perp}/E'_{\parallel}$) of PP composites from DMTA.

Morphology and Orientation

SEM images show that fibers are oriented in the direction of flow in the skin zones and are more randomly oriented in the core zone (skin/core effect in the fountain flow of the injection molding process).

Figure 16a evidences the fiber orientation in the skin and core of GF50 after a transversal fracture in the direction of cross flow. In the Figure 16b, the fracture surface of GF50 after longitudinal break in the direction of the flow injection is depicted.

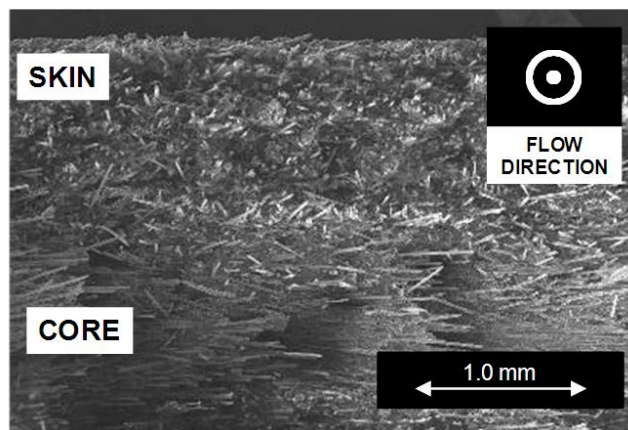


Figure 16a. SEM micrograph of GF50 (transversal fracture - cross flow direction).

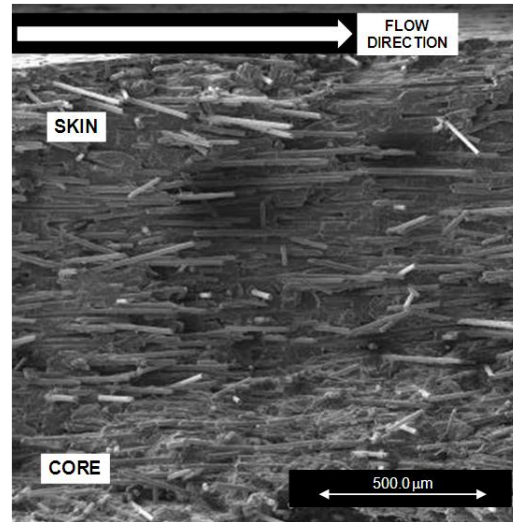


Figure 16b SEM micrographs of GF50 (longitudinal fracture-along flow direction).

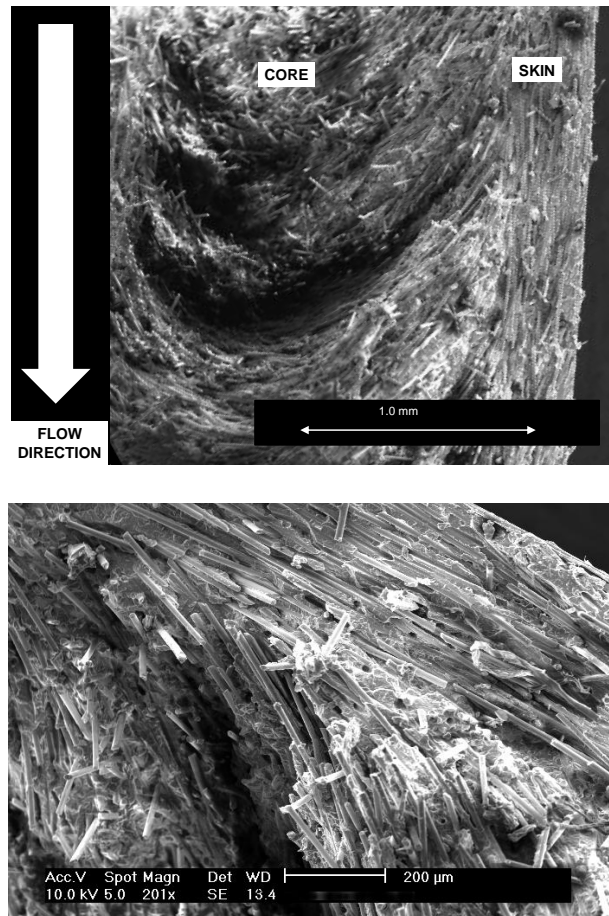


Figure 17. SEM micrographs of GF60 (longitudinal fracture-along flow direction).

Figures 17 show the fracture surface of GF60 after a longitudinal fracture in the direction of flow injection.

Fiber orientations in the core and in the skin layer are evidenced at different magnifications.

Flammability Test

To compare the effect of short glass fiber on the combustion of PP composite, ISO specimens were properly tested using an apparatus for LOI Analysis according to ASTM D-2863-06. Both polypropylene and its composites evidenced a LOI value lower than 0.19, as reported in literature [62-63].

Three different atmospheres with oxygen content of 19-21-23% were selected. Figure 18 shows the specimens of PP matrix and glass fiber composites after 180 seconds of the combustion test at 19% of oxygen.

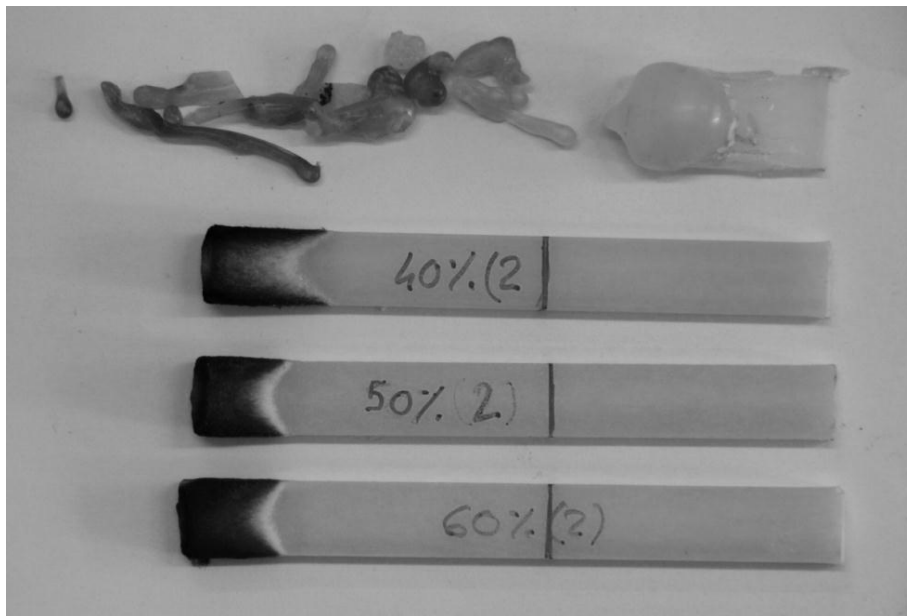


Figure 18. PP and GF-PP (40-50-60 % by wt.) specimens after 180 seconds of burning test in atmosphere with 19% of oxygen.

The rate of propagation of the advancing flame was evaluated for all materials, as shown in Figure 19 in the case of PP and GF40.

It is well evident that the propagation rate increases with the oxygen content and decreases with the presence of glass fibers. In particular, the flame propagation rate in short glass fiber composite decreases at about one-third of the polypropylene in various conditions of oxygen content, almost independently on the glass content (Table 7).

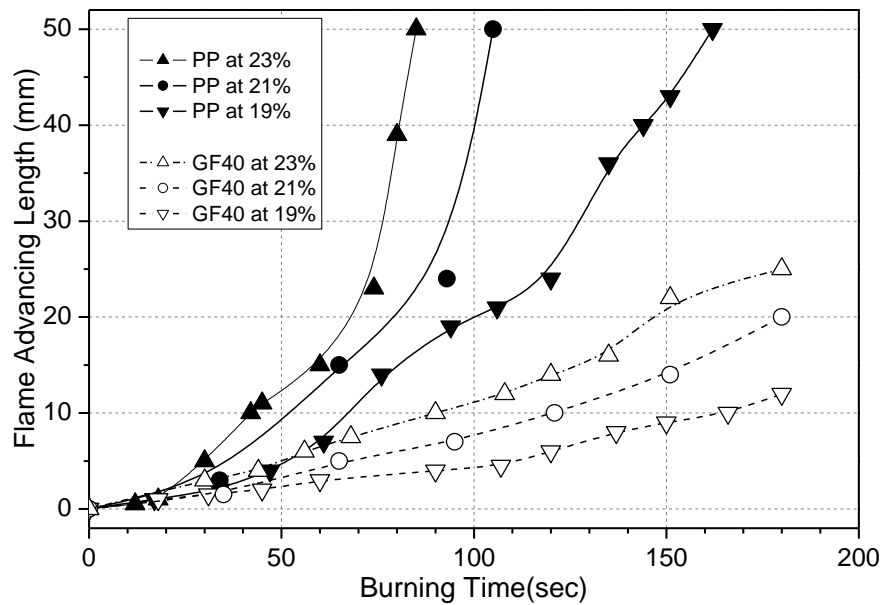


Figure 19. Length of the burned specimen vs. time of burning in flammability test for PP and PP-GF40 at various oxygen content.

Table 7. Propagation rate of PP matrix and GF composites as function of the percentage of oxygen in candle-like combustion (ASTM D2863-06)

Propagation rate (mm/sec)	PP	GF40	GF50	GF60
Oxygen Content (%)				
19	0.28	0.06	0.07	0.07
21	0.36	0.10	0.11	0.11
23	0.39	0.13	0.13	0.15

CONCLUSION

High load polypropylene composite containing talc, calcium carbonate and short glass fibers up to 60%, 80% and 65% by wt., respectively, were produced by compounding with a relatively low viscosity polymer matrix. All materials exhibited adequate flowability for injection molding processes. Significant increase of stiffness and strength, with a reduction of deformation at break was found for all the composite composition. According to literature data, short glass fibers were progressively chopped during processing in both compounding and injection, reaching average length in between 0.2-0.5 mm, nonetheless keeping outstanding composite properties in particular stiffness and strength. In the same time, short glass fiber composite exhibited a higher toughness (Charpy impact values) at low temperature and heat deflection temperature in the range 148-152°C. Finally, anisotropy factor was evaluated for injection molded large plate.

Following these results, high load polypropylene composite recipes described here are produced in almost standard compounding machines (that is not true for LGF) and appear suitable for the production of articles via traditional injection molding equipment without any special tooling or gating (e.g. hot runner) that are required in the case of long fiber polypropylene composites.

REFERENCES

- [1] B. Pukansky, *Fillers for polypropylene, Particulate filled polypropylene, in "Polypropylene. An A-Z Reference"*, J. Karger-Kocsic ed., Kluwer Acad. Publish, Dordrecht – The Netherlands (1999).
- [2] P.F. Chu, Glass fiber-reinforced polypropylene, in *"Handbook of polypropylene and polypropylene composite"*, H.G. Karian ed., Marcel Dekker, New York, (1999).
- [3] A.G. Gibson, Processing and properties of reinforced polypropylene, in *"Polypropylene. Structure, blends and composites. Composites"* Vol 3, J. Karger-Kocsic ed., Chapman Hall, London (1995).
- [4] J.I. Kroschwitz, A. Seidel, *Kirk-Othmer, Encyclopedia of Chemical Technology*, V ed., Wiley-Interscience, Hoboken, NJ 2004-2007.
- [5] Lyondellbasell data (2011).
- [6] M. Akay, and D. Barkley, *Compos. Struct.* 3, 269 (1985).
- [7] V.B. Gupta, R.K. Mittal, P.K. Sharma, G. Mennig, and J. Wolters, *Polym. Comp.* 10,16 (1989).
- [8] M. Akay, and D. Barkley, *J. Mater. Sci.* 26, 2731 (1991).
- [9] S. Hashemi, and M. Koohgilani, *Polym. Eng. Sci.* 35, 1124 (1995).
- [10] J.L. Thomason, and M.A. Vlug, *Composites Part A* 27, 477 (1996).
- [11] J.L. Thomason, and M.A. Vlug, *Composites Part A* 28, 277 (1997).
- [12] S.Y. Fu, B. Lauke, E. Mader, X.Hu, and C.Y. Yue, *J. Mater. Proc. Techn.* 89, 501 (1999).
- [13] A. Pegoretti, and T. Riccò, *J. Comp. Mater.* 34,1009 (2000).
- [14] S.Y. Fu, B. Lauke, E. Mader, X.Hu, and C.Y. Yue, *Composites Part A* 31,1117 (2000).
- [15] J.L. Thomason, *Compos. Sci. Technol.* 62, 1455 (2002).
- [16] J.L. Thomason, *Composites Part A* 33, 1283 (2002).
- [17] A.P. Gupta, U.K. Saroop, G.S. Jha, and Minakshi Verma, *Polym.-Plast. Technol. Eng.* 42, 297 (2003).
- [18] C. Mobuchon, P.J. Carreau, M.C. Heuzey, M. Sepehr, and G. Ausias, *Polym. Comp.* 26, 247 (2005).
- [19] J.L. Thomason, *Composites Part A* 38, 210 (2007).
- [20] I. Taha, and Y.F. Abdin, *J. Composite Material* 45, 1805 (2011).
- [21] J. Denault, T. Vu-Khanh, and B. Foster, *Polym. Compos.* 10, 313 (1989)
- [22] P. Peltonen, E.J. Paakkonen, P.K. Jarvela, and P. Tormala, *Plast. Rubber Compos. Proc. Appl.* 23, 111 (1995).
- [23] J.L. Thomason, *Composites Part A* 33, 1641 (2002).
- [24] J. Hartikainen, M. Lindnerm, T. Harmia, and K. Friedrich, *Plast. Rubber Compos.* 33, 77 (2004).

-
- [25] J.L. Thomason, *Composites Part A* 36, 995 (2005).
- [26] K. Senthil Kumar, A.K. Ghosh, and N. Bhatnagar, *Polym. Compos.* 28, 259 (2007).
- [27] M. Rohde, A. Ebel, F. Wolff-Fabris, and V. Altstadt, *Int. Polym. Proc.* 26, 292 (2011).
- [28] J. Wang, C. Geng, F. Luo, Y. Liu, K. Wang, Q. Fu, and B. He, *Mater. Sci. Eng. A* 528, 3169 (2011).
- [29] B. He, H. Liu, J. Leng, B. Yang, X. Chen, J. Fu, and Q. Fu, *J. Reinf. Plast. Compos.* 30, 222 (2011).
- [30] D.V. Rosato, and D.V. Rosato, *Injection Molding Handbook: The Complete Molding Operation Technology, Performance, Economics*, 2nd Edition, Chapman and Hall, New York, (1995).
- [31] P.F. Bright, R.J. Crowson, and M.J. Folkes, *J. Mater. Sci.* 13, 2497 (1978).
- [32] M. Sanou, B. Chung, and C. Cohen *Polym. Eng. Sci.* 25, 1008 (1985).
- [33] P. Singh, and M.R. Kamal, *Polym. Compos.* 10, 344 (1989).
- [34] M. Gupta, and K.K. Wang, *Polym. Compos.* 14, 367 (1993).
- [35] S.Y. Fu, and B. Lauke, *Compos. Sci. Technol.* 56, 1179 (1996).
- [36] L. Averous, J.C. Quantin, A. Crespy, and D. Lafon, *Polym. Eng. Sci.* 37, 329 (1997).
- [37] J.P. Green, and J.O. Wilkes, *Polym. Eng.Sci.* 37, 1019 (1997).
- [38] H.G. Karian, and K. Stoops, *Polym. Compos.* 19, 31 (1998).
- [39] S.E. Barbosa, and J.M. Kenny, *J. Reinf. Plast. Compos.* 18, 413 (1999).
- [40] A. Larsen, *Polym. Compos.* 21, 51 (2000).
- [41] N. Sombatsompop, and W. Chaiwattanpipat, *Polym. Test.* 19, 713 (2000).
- [42] E.G. Kim, J.K. Park, and S.H. Jo, *J. Mater. Proc. Technol.* 111, 225 (2001).
- [43] P.J. Hine, and R.A. Duckett, *Polym. Compos.* 25, 237 (2004).
- [44] S. Patcharaphun, and G. Mennig, *Polym. Compos.* 26, 823 (2005)
- [45] W.N. Ota, S.C. Amico, and K.G. Satyanarayana, *Compos. Sci. Technol.* 65, 873 (2005).
- [46] C.A. Silva, J.C. Viana, F.W.J. van Hattum, and A.M. Cuhna, *J. Mater. Sci.* 42, 5203 (2007).
- [47] M. Benhadou, and A. Haddout, *J. Reinf. Plast. Compos.* 26, 1357 (2007).
- [48] J.P. Qu, X. Zhang, G. Jin, *Polym.-Plast. Technol. Eng.* 47, 186 (2008)
- [49] P. Onishi, and S. Hashemi, *J. Mater. Sci.* 44, 3445 (2009).
- [50] C. Yang, H.-X. Huang, and K. Li, *Polym. Compos.* 31, 1899 (2010).
- [51] R. Turkovic, and L. Erwin, *Polym. Eng. Sci.* 23, 743 (1983).
- [52] B. Franzen, C. Klason, J. Kubat and T. Kitano, *Composites* 20, 65 (1989)
- [53] V.B. Gupta, R.K. Mittal, P.K. Sharma, G. Mennig, and J. Wolters, *Polym. Compos.* 10, 8 (1989).
- [54] J.P. Hernandez, T. Raush, A. Rios, S. Strauss, and T.A. Osswald, *Eng. Anal. Bound. Elem.*, 26, 621 (2002).
- [55] G. Zhang, and M.R. Thompson, *Compos. Sci. Technol.* 65, 2240 (2005).
- [56] S. Patcharaphun, and G. Opaskornkul, *Kasetsart J. (Nat. Sci.)* 42, 392 (2008).
- [57] K.A. Geddes, R.A. Guyer, and R.C. Miller, High melt flow fiber reinforced propylene polymer compositions, *United States Patent* No. 4,997,875, Mar. 5, 1991.
- [58] Basell Poliolefine Italia srl, E. Masarati, E. Costantini, and M. Consalvi, Filled polyolefin compositions, *Patent WO 2008/074713*, June 26, 2008.
- [59] D.W. Van Krevelen, "Properties of Polymers", 3rd Ed., Elsevier, Amsterdam (1990).
- [60] J.C. Halpin, and J.L. Kardos, *Polym. Eng. Sci.* 18, 496 (1978).
- [61] P.K. Mallick, "Fiber Reinforced Composites", Marcel Dekker Inc., New York (1988).

-
- [62] H. Dvir, M. Gottlieb, S. Daren, and E. Tartakovsky, *Compos. Sci. Technol.* 63, 1865 (2003).
- [63] B. K. Kandola, and R. Toqueer-Ul-Haq, *Fire Mater.* (2011) - doi/10.1002/fam.1120/full